Cancer Chemother Pharmacol (2016) 77:565–573
DOI 10.1007/s00280-015-2945-y

ORIGINAL ARTICLE

Technetium Tc 99m sulfur colloid phenotypic probe for the pharmacokinetics and pharmacodynamics of PEGylated liposomal doxorubicin in women with ovarian cancer

Hugh Giovinazzo[1,2] · Parag Kumar[1,3] · Arif Sheikh[4] · Kristina M. Brooks[3] · Marija Ivanovic[4] · Mark Walsh[1] · Whitney P. Caron[1] · Richard J. Kowalsky[4] · Gina Song[1] · Ann Whitlow[4] · Daniel L. Clarke-Pearson[4,5,6] · Wendy R. Brewster[4,5,6] · Linda Van Le[4,5,6] · Beth A. Zamboni[7] · Victoria Bae-Jump[4,5,6] · Paola A. Gehrig[4,5,6] · William C. Zamboni[1,6,8,9,10]

Received: 10 August 2015 / Accepted: 11 December 2015 / Published online: 28 January 2016

Abstract
Purpose Significant variability in the pharmacokinetics and pharmacodynamics of PEGylated liposomal doxorubicin (PLD) exists. PLD undergoes clearance via the mononuclear phagocyte system (MPS). Technetium Tc 99m sulfur colloid (TSC) is approved for imaging MPS cells. We investigated TSC as a phenotypic probe of PLD pharmacokinetics and pharmacodynamics in women with epithelial ovarian cancer.
Methods TSC 10 mCi IVP was administered and followed by dynamic planar and SPECT/CT imaging and blood pharmacokinetics sampling. PLD 30–40 mg/m^2 IV was administered with or without carboplatin, followed by plasma pharmacokinetics sampling.
Results There was a linear relationship between TSC clearance and encapsulated doxorubicin clearance ($R^2 = 0.61$, $p = 0.02$), particularly in patients receiving PLD alone ($R^2 = 0.81$, $p = 0.04$). There was a positive relationship ($\rho = 0.81$, $p = 0.01$) between maximum grade palmar-plantar erythrodysesthesia toxicity developed and estimated encapsulated doxorubicin concentration in hands.
Conclusions TSC is a phenotypic probe for PLD pharmacokinetics and pharmacodynamics and may be used to individualize PLD therapy in ovarian cancer and for other nanoparticles in development.

Keywords Pharmacokinetics · Pharmacodynamics · Liposomes · TSC · PEGylated liposomal doxorubicin · Phenotypic probe · Ovarian cancer

Hugh Giovinazzo and Parag Kumar are co-primary authors.

Electronic supplementary material The online version of this article (doi:10.1007/s00280-015-2945-y) contains supplementary material, which is available to authorized users.

✉ William C. Zamboni
zamboni@email.unc.edu

[1] Division of Pharmacotherapy and Experimental Therapeutics, University of North Carolina at Chapel Hill-Eshelman School of Pharmacy, 120 Mason Farm Road, Suite 1013, CB 7361, Chapel Hill, NC 27599-7361, USA

[2] Department of Pharmacology and Molecular Sciences, Johns Hopkins School of Medicine, 725 N. Wolfe St., Baltimore, MD 21205, USA

[3] Clinical Pharmacokinetics Research Laboratory, National Institutes of Health, Clinical Center Pharmacy Department, 10 Center Drive Bldg. 10, 1C-240G, Bethesda, MD 20892, USA

[4] UNC School of Medicine, 321 S. Columbia St., Chapel Hill, NC 27599, USA

[5] Division of Gynecologic Oncology, Department of Obstetrics and Gynecology, UNC Lineberger Comprehensive Cancer Center, 103B Physicians' Office Building CB# 7572, Chapel Hill, NC 27599, USA

[6] UNC Lineberger Comprehensive Cancer Center, 101 Manning Drive, Chapel Hill, NC 27514, USA

[7] Department of Mathematics, Carlow University, Pittsburgh, PA, USA

[8] UNC Institute for Pharmacogenomics and Individualized Therapy, 120 Mason Farm Road, Chapel Hill, NC 27599, USA

[9] Carolina Center of Cancer Nanotechnology Excellence, 1079 Genetic Medicine Building, Chapel Hill, NC 27599, USA

[10] North Carolina Biomedical Innovation Network, 013 Genetic Medicine Building CB#7361, Chapel Hill, NC 27599, USA

Introduction

Doxil® is a commercially available formulation of doxorubicin encapsulated within a liposome with polyethylene glycol (PEG) molecules conjugated to the surface [1]. Doxil®, or PEGylated liposomal doxorubicin (PLD), is used clinically for the treatment of refractory epithelial ovarian cancer (EOC), multiple myeloma, AIDS-related Kaposi sarcoma, breast cancer, and various other malignancies. Delivering small molecule agents in liposomes modifies the pharmacokinetic (PK) and pharmacodynamic (PD) characteristics of the agent [2–4]. PLD has a longer plasma half-life ($t_{1/2}$) (>14-fold), larger area under the concentration–time curve (AUC) (>30,000-fold), and a smaller volume of distribution (Vd) (~1800-fold) compared with non-liposomal, small molecule doxorubicin [5–7]. These characteristics may improve efficacy and explain PLD's altered toxicity profile [i.e., reduced cardiotoxicity and development of palmar-plantar erythrodysesthesia (PPE)]. Non-PEGylated liposomal agents are rapidly cleared by the mononuclear phagocyte system (MPS), consisting primarily of monocytes and macrophages in the blood, liver, and spleen. Newer liposomal agents, such as PLD, are formulated with lipids conjugated to PEG, which reduces recognition by the MPS and prolongs circulation and exposure to these agents [2, 5–7]. However, PEG liposomes are still cleared via uptake by the MPS.

A phenotypic probe is a test that can be administered to a patient as a potential indicator of a drug's PK or PD, which can then be used to individualize therapy [8]. Technetium Tc 99m sulfur colloid injection (TSC) is a radioactive colloidal dispersion of Tc_2S_7 incorporated into sulfur particles [9]. TSC is approved by the FDA for imaging the liver, spleen, and bone marrow. Tc(99m) decays with a $t_{1/2}$ of ~6 h. After intravenous injection, TSC clears from the vasculature by phagocytosis via MPS cells, distribution to second and third compartments (e.g., tissues, ascites, and pleural effusion), and other potential pathways with an elimination $t_{1/2}$ of ~2.5 min [9–11]. In a healthy individual, 80–90 % of the TSC dose is rapidly localized in the liver and 4–8 % in the spleen [12]. Uptake of TSC in liver and spleen reflects both the distribution and presence of functioning MPS cells in these organs and the extent of hepatic and splenic blood flow [13].

The assessment of radiopharmaceutical agents as phenotypic probes for the PK and PD of therapeutic agents has been successfully deployed in various clinical trials with relatively small cohorts. Koukourakis et al. [14] formulated Tc(99m)-radiolabelled liposomal doxorubicin and demonstrated increased accumulation in a cohort of 10 patients with metastatic brain tumors and 5 patients with glioblastoma. In addition, radiopharmaceuticals can be used as a theranostic agent, as demonstrated by Stopar et al. [15] where 10 patients with B cell non-Hodgkin's lymphoma were given Tc(99m)-labeled rituximab. The results from this trial demonstrated that the Tc(99m)-labeled rituximab accumulated in CT-confirmed CD20 + NHL sites. Furthermore, the hepatobiliary imaging agent Tc(99m) mebrofenin was used by Pfeifer et al. [16] to develop a semi-physiologically based PK model for the transporter-mediated drug–drug interactions due to orally administered ritonavir in 8 and 10 healthy volunteers.

The decreased cardiotoxicity profile of PLD is thought to be due to the decreased distribution of doxorubicin to the heart [5–7, 17, 18]. While cardiotoxicity is decreased, new toxicities may arise when compared to conventional doxorubicin [19–21]. The most predominant of these is palmar-plantar erythrodysesthesia (PPE), also known as hand-foot syndrome [20, 22–24]. PPE is characterized by erythema, swelling, tenderness, and pain with associated peeling, blistering, and ulceration on the palms of hands and soles of the feet. The exact mechanisms and risk factors associated with PPE are unknown. However, several pathophysiological mechanisms have been suggested. These include higher susceptibility of keratinocytes due to high turnover rate, anatomic differences such as high density of sweat glands and thicker stratum corneum, physical friction or trauma resulting in extensive capillary blood flow, immune-mediated inflammatory reactions, and metal ions in the skin contributing to increased production of free radicals in the presence of PLD [25, 26]. Additional risk factors for the development of PPE include increased dose, frequency, and prolonged drug circulation of anthracyclines, which contribute to increased drug accumulation in cutaneous tissues [27].

Liposomal agents have been shown to have significantly greater PK variability than small molecule, non-liposomal agents [28]. PLD has high and clinically relevant interpatient PK variability, which may be related to variability in patients' MPS function [28–30]. In theory, the interpatient variability in MPS function and PLD PK may be a major factor responsible for variability in the PD (efficacy and toxicity) observed with PLD. Thus, there is a need to identify, profile, and phenotypically measure the factors associated with this variability [31]. This is the first study to evaluate the use of TSC as a phenotypic probe for the PK and PD disposition of any nanoparticle agent and specifically for PLD in patients with EOC.

Materials and methods

Patient eligibility

Women ≥18 years of age receiving PLD ± carboplatin for EOC treatment were eligible. Exclusion criteria consisted of women who were pregnant or breast-feeding. This study was approved by the University of North Carolina Institutional Review Board, and all patients were provided written informed consent prior to enrollment.

TSC imaging and PK studies

TSC administration, imaging, and PK studies were completed prior to administration of PLD ± carboplatin as part of standard clinical treatment for EOC. On day 7 to 1 before cycle 1 day 1 of PLD therapy, TSC was administered at 10 mCi IV push × 1. Blood samples (3 mL) were collected prior to administration, and at 2, 5, 10, 15, 30, and 60 min after TSC. The activity of TSC in blood was measured using a gamma scintillation well counter within 2 h of sample collection [13]. The decay-corrected samples were recorded as counts per minute (CPM) using a Caprac-R Well Counter (Capintec, Inc.).

Anterior and posterior images of the liver and spleen were obtained every 10 s for 10 min after TSC. Hand images were taken at a single imaging time point within 10 min after the end of the serial liver and spleen images. The geometric means of the counts recorded in the anterior and posterior images of the liver, spleen, and hands were calculated at each image time point (Siemens Software Inc.). SPECT imaging was then obtained along with low-dose, non-contrasted transmission axial CT images over the same region for the purpose of anatomic localization (Siemens Symbia T6 SPECT-CT system) [32]. Liver, spleen, and hand scintigraphic volumes were obtained by drawing and region of interest (ROI) off the SPECT images, and the geometric mean count divided by this volume was used to quantify the concentration of TSC in the ROI on the SPECT-CT images.

PLD dose and administration

PLD was administered as an IV infusion over 1–2 h every 28 days at a dose of 40 mg/m^2 in patients receiving PLD alone or 30 mg/m^2 in patients receiving concurrent carboplatin (AUC = 5 mg/mL/min). Regimen selection was not altered for the purpose of this study.

PLD PK studies

For PK studies of PLD, serial blood samples (5 mL) were obtained prior to PLD administration, at the end of infusion, and at 2 h, 6 h, 24 h, 48 h, 72 h, 96 h, 168 h, and on day 28 after cycle 1 of PLD therapy. Plasma was processed to measure encapsulated and released doxorubicin using solid-phase separation and HPLC with fluorescence detection as previously described [33–35].

PK analyses

PK parameters of area under the plasma concentration versus time curve (AUC), clearance (CL), half-life ($t_{1/2}$), and volume of distribution (Vd) for TSC in blood, liposomal encapsulated doxorubicin in plasma, and released doxorubicin in plasma were calculated using non-compartmental methods (Phoenix WinNonlin® v. 6·02, Pharsight Corp). AUC was computed via the "linear-up-log-down trapezoidal" rule, and CL of TSC and PLD in the blood was calculated by the equation CL = Dose/AUC. The relationship between CL of TSC in blood and PLD in plasma was evaluated.

Patient toxicity assessment

PPE toxicity was assessed throughout the entire duration of PLD therapy cycles for each patient. The grade of PPE toxicity was determined by the principle investigator using the National Cancer Institute's Common Terminology Criteria for Adverse Events (v4·03).

Sample size calculations and statistical analysis

Sample size calculations were performed using SAS Power and Sample Size 3.1. The primary outcomes were clearance and toxicity. Sample size was determined based on a two-sided 0.05 level Fisher's z test for a Pearson correlation coefficient of 0.80. Power was set at 80, 85, and 90 %. The corresponding sample sizes were 8, 9, and 10, respectively.

Linear regression analysis was used to test the statistical significance of the correlative relationship between PLD plasma clearance and TSC blood clearance. Spearman's correlation (SC) analysis was used to test the statistical significance of the correlation between estimated PLD concentrations in hands and maximum grade of PPE toxicity developed.

Results

Patient demographics

Ten women were enrolled on this study. Six patients received PLD alone at a dose of 40 mg/m^2, and four received PLD at a dose of 30 mg/m^2 in combination with carboplatin. Baseline patient characteristics are included in Table 1. Complete TSC and PLD PK data were available

Table 1 Patient characteristics upon enrollment

Characteristic	$n = 10$
Age (years)	
Mean	58.9
Range (min–max)	44–75
Race (*n*)	
Caucasian	9
African-American	1
Height (cm)	
Mean	165.9
Range (min–max)	157–178
Weight (kg)	
Mean	78.5
Range (min–max)	48–116
BMI (kg/m^2)	
Mean	28.7
Range (min–max)	19–42
BSA (m^2)	
Mean	1.83
Range (min–max)	1.46–2.0
Regimen (*n*)	
PLD 30 mg/m^2 + carboplatin	4
PLD 40 mg/m^2	6

for all patients with the exception of two patients where PLD PK samples were not obtained on days 8 and/or 28. A summary of PK parameters of TSC in blood and PK parameters for encapsulated and released doxorubicin in plasma is included in Table 2. Additionally, one patient was not included in the PPE toxicity analysis because TSC hand images were unsuccessfully captured due to equipment error.

TSC pharmacokinetics

The concentration versus time profiles of TSC in blood, liver, spleen, and hands are presented in Fig. 1a–d. TSC radioactivity versus time profiles in blood demonstrated a rapid decrease in radioactivity concentration in the blood within approximately 1 h (Fig. 1a). TSC radioactivity versus time profiles in the liver, spleen, and hands demonstrate rapid uptake of TSC and increases in radioactivity in the liver and spleen within 10 min (Fig. 1b, c). Mean TSC concentration in the liver was similar to mean concentration in spleen over the first 10 min post-TSC administration. The nearly equivalent concentration of TSC in the liver and spleen is consistent with the known biodistribution profile of TSC, as the volume of the spleen is roughly tenfold smaller than that of the liver and thus the amount of TSC distributed to the liver is approximately tenfold higher than to the spleen. There was significantly higher interpatient variability observed in the TSC concentration versus time profiles in spleen than in the liver. Interestingly, patients with higher liver TSC exposures did not demonstrate higher spleen TSC exposures. TSC concentration in the hands was measured at a single time point after administration and was approximately 2.6-fold lower than the mean TSC blood concentrations. The concentration of TSC in patients' hands was highly variable and was unrelated to TSC exposure in blood (Fig. 1d).

PLD pharmacokinetics

PLD PK sampling was completed for 10 women. Encapsulated and released doxorubicin concentration versus time profiles in plasma are shown in Fig. 2. In all patients, the peak encapsulated doxorubicin concentration in plasma was approximately tenfold greater than the peak released doxorubicin concentration. Additionally, encapsulated doxorubicin concentrations were detectable for up to 8 days after PLD administration in nearly all patients and up to 28 days after PLD administration in four patients. The released doxorubicin concentration versus time profile was found to closely mirror that of the encapsulated doxorubicin, but at a significantly lower concentration. Significant interpatient PK variability was observed for both the encapsulated and released doxorubicin PK disposition. The mean ± SD AUC for encapsulated and released doxorubicin was 2,353,223 ± 704,711 ng/mL * h and 243,541 ± 171,578 ng/mL * h, respectively. The mean ± SD ratio of released doxorubicin AUC to encapsulated doxorubicin AUC was 0.10 ± 0.05.

Table 2 PLD and TSC PK parameters ($n = 8$)

Parameter	Doxorubicin			Tc(99m)
	Released	Encapsulated	Released/encapsulated	
CL (mL/h)	253.0 (175.8)	25.7 (12.1)	–	20,545 (7986)
AUC (ng/mL * h)	243,541 (171,578)	2,898,782 (974,518)	0.10 (0.05)	432.2 (200.1)[a]
t½ (h)	189.7 (252.6)	79.6 (25.3)	–	0.38 (0.10)
Vd (mL)	401,66 (34,838)	2569 (502)	–	11,000 (4100)

Data presented as mean (SD)

[a] Units = nCi/mL * h

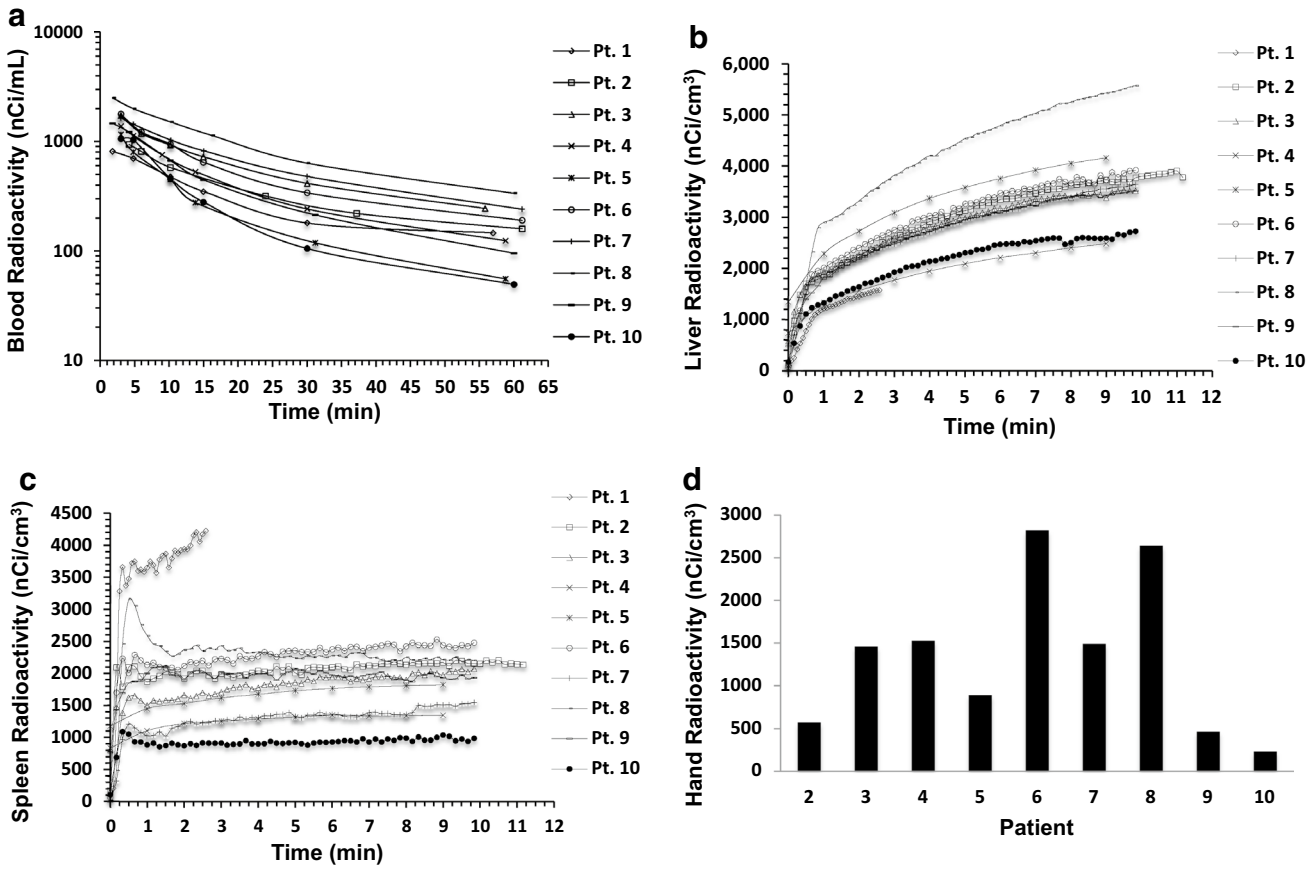

Fig. 1 Tc(99m) radioactivity versus time profiles in **a** blood ($n = 10$), **b** liver ($n = 10$), **c** spleen ($n = 10$), and **d** hands ($n = 9$) following administration of TSC

Relationship between TSC blood PK and encapsulated doxorubicin plasma PK

A direct linear relationship was found between the clearance of TSC in blood and clearance of encapsulated doxorubicin in plasma in all patients ($R^2 = 0.61$, $p = 0.02$) (Fig. 3a). In patients treated with PLD alone, there was a stronger direct linear relationship between the clearance of TSC in blood and clearance of encapsulated doxorubicin in plasma ($R^2 = 0.81$, $p = 0.04$) (Fig. 3b).

Relationship between estimated encapsulated doxorubicin hand concentration and PPE toxicity

An equation to estimate the encapsulated doxorubicin concentration in the patients' hands was developed based on data showing TSC CL from blood correlated with encapsulated doxorubicin CL from plasma (Online Resource Supplemental Equation (SE) 1). The final results on the relationship between TSC CL in blood and encapsulated doxorubicin CL in plasma are presented in the results section (Fig. 3). Using the variables attained by this study (TSC $\text{Concentration}_{\text{Hand}}$, TSC $\text{AUC}_{\text{Blood}}$, and encapsulated doxorubicin $\text{AUC}_{\text{Plasma}}$), the estimated encapsulated doxorubicin concentration in the hands was calculated (Online Resource SE2) and was compared to the maximum grade of PPE toxicity experienced by patients.

In order for TSC to be considered a viable phenotypic probe, it would ideally be capable of predicting the development of PPE by administering TSC prior to the administration of PLD, and thus not requiring measurement of PLD plasma exposure. Thus, we tested the ability of TSC to accomplish this by utilizing the preliminary finding of an association between TSC blood clearance and encapsulated doxorubicin plasma clearance to estimate the encapsulated doxorubicin $\text{AUC}_{\text{Plasma}}$ from the measured value of TSC $\text{AUC}_{\text{Blood}}$ obtained in the study. This was performed using the equation (encapsulated doxorubicin $\text{AUC}_{\text{Plasma}} = 21{,}138 \text{ X TSC } \text{AUC}_{\text{Blood}} + 1{,}641{,}403$). We then used this *de novo* estimated encapsulated doxorubicin $\text{AUC}_{\text{Plasma}}$ value to estimate the encapsulated doxorubicin concentration in the hands prior to PLD administration

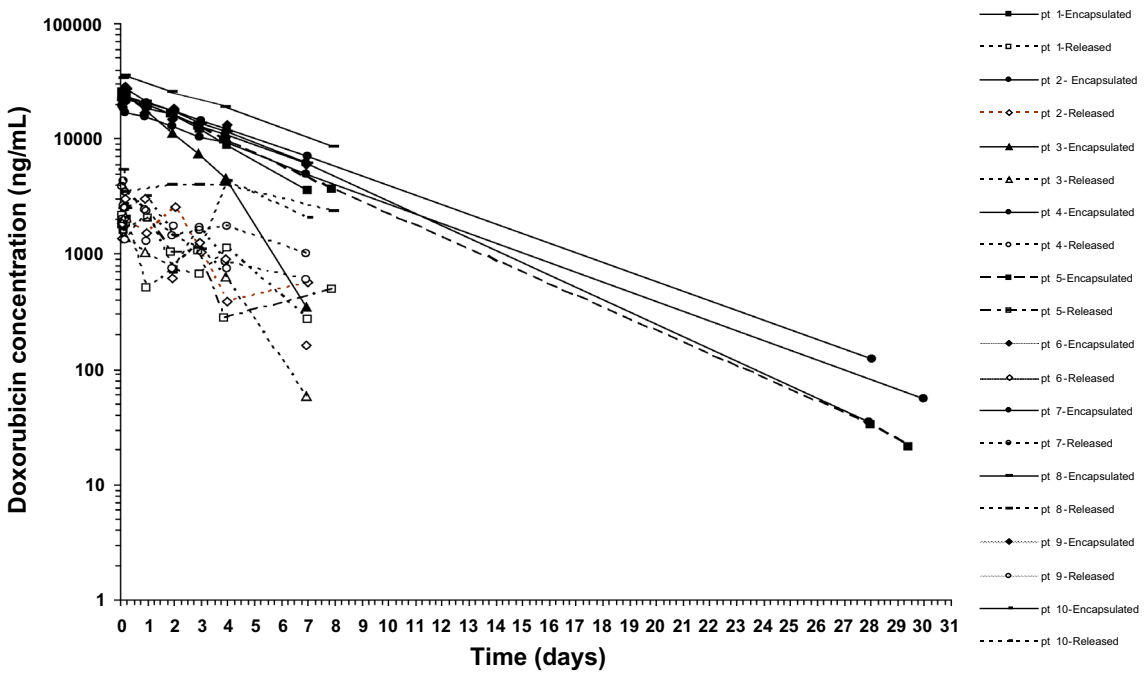

Fig. 2 Encapsulated and released doxorubicin concentration versus time profiles in plasma of patients ($n = 10$) following administration of PLD 40 mg/m^2 alone or Doxil 30 mg/m^2 in combination with carboplatin AUC = 5 mg/mL * min. Only data greater than LLOQ of encapsulated (300 ng/mL) and released (50 ng/mL) doxorubicin are presented

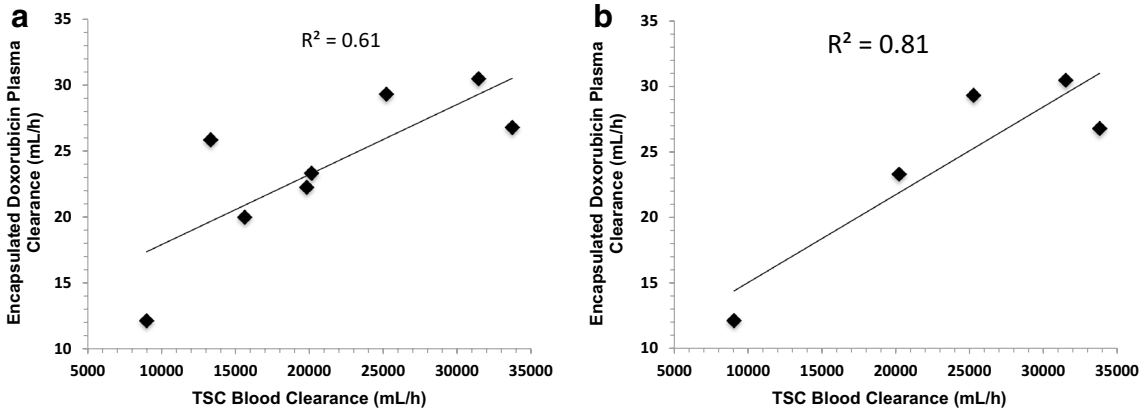

Fig. 3 Relationship between TSC blood clearance and encapsulated doxorubicin plasma clearance. A direct linear relationship was found between the plasma clearance of encapsulated doxorubicin and the blood clearance of TSC for all patients ($n = 8$)

(Online Resource SE3). This estimated concentration of encapsulated doxorubicin in the patients' hands using SE3 was then compared to the maximum grade of PPE toxicity.

Spearman's Correlation (SC) analysis demonstrated that there was a positive relationship between the estimated encapsulated doxorubicin concentration in patients' hands and the maximum grade of PPE toxicity developed ($\rho = 0.81$, $p = 0.01$) using measured encapsulated doxorubicin in plasma (Fig. 4a). Furthermore, TSC was evaluated as a phenotypic probe to calculate an estimated encapsulated doxorubicin AUC_{Plasma} from the TSC AUC_{Blood} obtained in the study in lieu of directly measuring encapsulated doxorubicin concentration in plasma. This method demonstrated a similar positive relationship between estimated encapsulated doxorbucin concentrations in patients' hands and the maximum grade of PPE toxicity

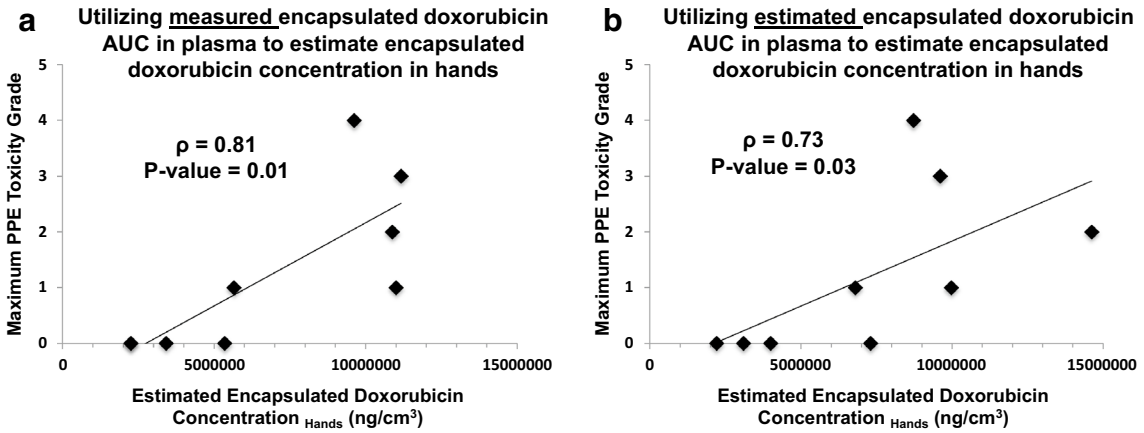

Fig. 4 Relationship between estimated encapsulated doxorubicin concentration in hands and maximum PPE toxicity. Using Spearman's correlation, there was a direct positive relationship between the maximum PPE toxicity grade developed in patients ($n = 9$) and the estimated encapsulated doxorubicin concentrations in the hands utilizing **a** measured encapsulated doxorubicin AUC in plasma and **b** measured TSC AUC in blood

developed using estimated encapsulated doxorubicin AUC in plasma from the TSC probe PK parameters ($\rho = 0.73$, $p = 0.03$) (Fig. 4b).

Discussion

The interindividual PK variability of PLD and other liposomal agents is clinically significant and greater than small molecule, non-liposomal doxorubicin [5–7]. This variability in exposure is thought to be associated with the variable efficacy and toxicity observed with therapy. Clearance of PEGylated and non-PEGylated liposomal and nanoparticle agents, such as PLD, occurs via the MPS [2, 6]. Due to these interactions, PK variability and PD variability of PLD are thought to be related to variability in the function of the MPS in patients. Thus, there is a need to evaluate the factors driving this variability and attempt to predict this variability in order to optimize treatment with PLD and other novel nanoparticle agents in patients with EOC and other diseases. Phenotypic probes are tests that can be administered to a patient as potential indicators of a drug's PK and PD, and subsequently can be used to individualize therapy. TSC is approved by the FDA for imaging areas of functioning cells of the MPS in the liver, spleen, and bone marrow. We therefore undertook the first study evaluating the use of TSC as a phenotypic probe for the PK and PD disposition of PLD in women with EOC.

Similar to findings in previous studies, significant interpatient variability in the PK of encapsulated and released doxorubicin was observed in our study [7]. Encapsulated doxorubicin concentrations were approximately tenfold greater than released doxorubicin concentrations in all patients. Significant interpatient PK variability was also observed for TSC in blood, liver, spleen, and patients' hands. Additionally, TSC concentrations in all organs and tissues evaluated within a patient were not similar and were unrelated. These findings suggest that differences in MPS within tissues as measured by TSC levels are consistent with the high PK variability observed with liposomal and nanoparticle agents.

Our results demonstrated a positive linear relationship between the blood clearance of TSC and plasma clearance of encapsulated doxorubicin ($R^2 = 0.61$, $p = 0.02$) (Fig. 3), especially those patients receiving PLD alone ($R^2 = 0.81$, $p = 0.04$). This suggests that the MPS is involved in the clearance of a wide variety of nanoparticles. In addition, the ability of TSC to better predict the clearance of PLD when given alone compared with PLD + carboplatin suggests that carboplatin may be altering MPS function. Consistent with our results, prior studies have reported modulation of monocyte function and chemotaxis by platinum agents, which may lead to an alteration in the plasma clearance of PLD by the MPS when carboplatin is co-administered [36]. These results also suggest that the TSC probe can be used to evaluate potential drug interactions related to MPS function and nanoparticle PK.

The estimated encapsulated doxorubicin concentration in hands using measured exposures of PLD in plasma was demonstrated to have a positive relationship with the maximum grade of PPE toxicity in patients (SC, $\rho = 0.81$, $p = 0.01$) (Fig. 4a). A similar relationship was also found by estimating the exposures of PLD in plasma and hands using TSC PK parameters (SC, $\rho = 0.73$, $p = 0.03$) (Fig. 4b). This demonstrates the ability to use TSC as a phenotypic probe for predicting the development and severity of PPE toxicity prior to administration of PLD. The lack

of a relationship between TSC AUC in blood and TSC concentrations in patients' hands suggests that the presence of MPS cells in the hands is important in determining the distribution of PLD to tissues instead of solely the exposure in plasma. Moreover, our data suggest that the presence of MPS cells in the hand may be a mechanism associated with the development of PPE toxicity. Previous studies have shown that PLD-associated PPE may arise from inflammatory reactions mediated by macrophage antigen presentation and subsequent cytotoxic T cell and natural killer cell activation, along with upregulation of tumor necrosis factor (TNF) and CD95 in the epidermis [25, 27, 37, 38]. Thus, TSC could be used as a phenotypic probe to measure the presence of MPS cells in the hands and predict the occurrence and severity of PPE in patients.

The results of our study demonstrate that TSC may be used as a phenotypic probe to predict PLD PK (plasma clearance and exposure in patients' hands) and PD (development of PPE toxicity) in individual patients prior to PLD administration. These results are somewhat surprising considering the large structural and chemical differences between TSC and PLD. However, these differences demonstrate the apparent non-specificity of the MPS in the uptake and clearance of nanoparticles and particles of different sizes. In addition, these results suggest that the clearance of nanoparticles with different chemical (e.g., non-PEGylated vs. PEGylated liposomes) and PK characteristics (e.g., high, medium and low clearance) in patients will have the same rank order of clearance in patients. Thus, the measured clearance rate of one type of nanoparticle in a patient can be used to predict the clearance of another distinct nanoparticle.

These results have strong clinical and developmental implications about the future use of TSC or other nanoparticle imaging agents as phenotypic probes of MPS function, PLD PK and PD, and the ability to potentially individualize PLD therapy in EOC and other cancers. In addition, due to the development of numerous other liposomal and nanoparticle agents that are cleared via the MPS, the potential ability of TSC to predict the PK and PD of other nanoparticle agents could be critical to the translational development and clinical success of future novel therapies. Ultimately, TSC may be used to screen the MPS activity in patients prior to receiving nanoparticle chemotherapy to allow for individualized dosing as a method to optimize efficacy while minimizing toxicity. Patients with lower MPS activity may be at risk of increased drug exposure and adverse events and thus require lower doses of PLD, whereas patients with higher MPS activity may require higher or more frequent doses in order to achieve optimal treatment response. The use of TSC is highly translatable and readily transferrable to clinical practice as TSC is already FDA-approved and used clinically for imaging of MPS-related organs, and gamma cameras and counters are readily available in hospitals and imaging centers. Further studies validating the ability of TSC to perform as a reliable phenotypic probe of the MPS and to potentially individualize the therapy of other nanoparticle agents are warranted.

Acknowledgments This study was funded by the Lineberger Comprehensive Cancer Center, UNC University Cancer Research Fund (UCRF) and the Carolina Center of Cancer Nanotechnology Excellence (C-CCNE) Pilot grant (NIH/NCI CA119343). The investigators would like to thank the faculty and staff of the UNC School of Medicine, Divisions of Gynecologic Oncology and Nuclear Medicine; UNC North Carolina Translational and Clinical Sciences Institute, Clinical and Translational Research Center; UNC Eshelman School of Pharmacy, Translational Oncology and Nanoparticle Drug Development Initiative Lab; the CCNE; and the patients, families, and friends who made this work possible.

Compliance with ethical standards

Conflict of interest The authors declare that they have no conflict of interest.

Research involving human participants All procedures performed in studies involving human participants were in accordance with the ethical standards of the institutional and/or national research committee and with the 1964 Helsinki Declaration and its later amendments or comparable ethical standards.

Informed consent Informed consent was obtained from all individual participants included in the study.

References

1. Centocor Ortho Biotech Products (2011) Doxil® (doxorubicin HCl liposome injection) package insert. Raritan, NJ
2. Drummond DC, Meyer O, Hong K, Kirpotin DB, Papahadjopoulos D (1999) Optimizing liposomes for delivery of chemotherapeutic agents to solid tumors. Pharmacol Rev 51(4):691–743
3. Papahadjopoulos D, Allen TM, Gabizon A, Mayhew E, Matthay K, Huang SK, Lee KD, Woodle MC, Lasic DD, Redemann C (1991) Sterically stabilized liposomes: improvements in pharmacokinetics and antitumor therapeutic efficacy. Proc Natl Acad Sci USA 88(24):11460–11464
4. Woodle MC, Lasic DD (1992) Sterically stabilized liposomes. Biochim Biophys Acta 1113(2):171–199
5. Allen TM, Stuart DD (1999) Liposomal pharmacokinetics: classical, sterically stabilized, cationic liposomes and immunoliposomes. In: Janoff AS (ed) Liposomes: rational design. Marcel Dekker, New York
6. Allen TM, Hansen C (1991) Pharmacokinetics of stealth versus conventional liposomes: effect of dose. Biochim Biophys Acta 1068(2):133–141
7. Working PK, Newman MS, Huang SK, Mayhew E, Vaage J, Lasic DD (1994) Pharmacokinetics, biodistribution and therapeutic efficacy of doxorubicin encapsulated in Stealth® liposomes (Doxil®). J Liposome Res 4(1):667–687
8. Kalvass JC, Graff CL, Pollack GM (2004) Use of loperamide as a phenotypic probe of mdr1a status in CF-1 mice. Pharm Res 21(10):1867–1870
9. Pharmalucence (2012) Package insert for kit for the preparation of technetium Tc 99m sulfur colloid injection diagnostic for intravenous and oral use. Billerica, MA

10. Shih WJ, Domstad PA, DeLand FH, Purcell M (1985) Simultaneous demonstration of pleural effusion and ascites by technetium-99 m sulfur colloid liver-spleen scintigraphy. Clin Nucl Med 10(9):637–638
11. Shih WJ, Domstad PA, Friedman B, DeLand FH (1986) Intrathoracic abnormalities demonstrated by technetium-99 m sulfur colloid imaging. Clin Nucl Med 11(11):792–796
12. Kowalsky RJ, Falen SW (2004) Radiopharmaceuticals in nuclear pharmacy and nuclear medicine. In: 3rd edn. American Pharmacists Association, Washington, p 199
13. Seidner DL, Mascioli EA, Istfan NW, Porter KA, Selleck K, Blackburn GL, Bistrian BR (1989) Effects of long-chain triglyceride emulsions on reticuloendothelial system function in humans. J Parenter Enteral Nutr 13(6):614–619
14. Koukourakis MI, Koukouraki S, Giatromanolaki A, Archimandritis SC, Skarlatos J, Beroukas K, Bizakis JG, Retalis G, Karkavitsas N, Helidonis ES (1999) Liposomal doxorubicin and conventionally fractionated radiotherapy in the treatment of locally advanced non-small-cell lung cancer and head and neck cancer. J Clin Oncol 17(11):3512–3521
15. Gmeiner Stopar T, Fettich J, Zver S, Mlinaric-Rascan I, Hojker S, Socan A, Peitl PK, Mather S (2008) 99 mTc-labelled rituximab, a new non-Hodgkin's lymphoma imaging agent: first clinical experience. Nucl Med Commun 29(12):1059–1065. doi:10.1097/MNM.0b013e3283134d6e
16. Pfeifer ND, Goss SL, Swift B, Ghibellini G, Ivanovic M, Heizer WD, Gangarosa LM, Brouwer KL (2013) Effect of ritonavir on (99 m) technetium–mebrofenin disposition in humans: a semi-PBPK modeling and in vitro approach to predict transporter-mediated DDIs. CPT Pharmacomet Syst Pharmacol 2:20. doi:10.1038/psp.2012.21
17. Newman MS, Colbern GT, Working PK, Engbers C, Amantea MA (1999) Comparative pharmacokinetics, tissue distribution, and therapeutic effectiveness of cisplatin encapsulated in long-circulating, pegylated liposomes (SPI-077) in tumor-bearing mice. Cancer Chemother Pharmacol 43(1):1–7. doi:10.1007/s002800050855
18. Zamboni WC, Gervais AC, Egorin MJ, Schellens JH, Zuhowski EG, Pluim D, Joseph E, Hamburger DR, Working PK, Colbern G, Tonda ME, Potter DM, Eiseman JL (2004) Systemic and tumor disposition of platinum after administration of cisplatin or STEALTH liposomal-cisplatin formulations (SPI-077 and SPI-077 B103) in a preclinical tumor model of melanoma. Cancer Chemother Pharmacol 53(4):329–336. doi:10.1007/s00280-003-0719-4
19. Cattel L, Ceruti M, Dosio F (2004) From conventional to stealth liposomes: a new frontier in cancer chemotherapy. J Chemother (Florence, Italy) 16(Suppl 4):94–97. doi:10.1179/joc.2004.16.4.94
20. Rose PG (2005) Pegylated liposomal doxorubicin: optimizing the dosing schedule in ovarian cancer. Oncologist 10(3):205–214. doi:10.1634/theoncologist.10-3-205
21. Vail DM, Amantea MA, Colbern GT, Martin FJ, Hilger RA, Working PK (2004) Pegylated liposomal doxorubicin: proof of principle using preclinical animal models and pharmacokinetic studies. Semin Oncol 31(6 Suppl 13):16–35
22. Krown SE, Northfelt DW, Osoba D, Stewart JS (2004) Use of liposomal anthracyclines in Kaposi's sarcoma. Semin Oncol 31(6 Suppl 13):36–52
23. Maeda H, Wu J, Sawa T, Matsumura Y, Hori K (2000) Tumor vascular permeability and the EPR effect in macromolecular therapeutics: a review. J Control Release 65(1–2):271–284. doi:10.1016/S0168-3659(99)00248-5
24. Markman M, Gordon AN, McGuire WP, Muggia FM (2004) Liposomal anthracycline treatment for ovarian cancer. Semin Oncol 31(6 Suppl 13):91–105
25. Martschick A, Sehouli J, Patzelt A, Richter H, Jacobi U, Oskay-Ozcelik G, Sterry W, Lademann J (2009) The pathogenetic mechanism of anthracycline-induced palmar-plantar erythrodysesthesia. Anticancer Res 29(6):2307–2313
26. Yokomichi N, Nagasawa T, Coler-Reilly A, Suzuki H, Kubota Y, Yoshioka R, Tozawa A, Suzuki N, Yamaguchi Y (2013) Pathogenesis of hand-foot syndrome induced by PEG-modified liposomal doxorubicin. Hum Cell 26(1):8–18. doi:10.1007/s13577-012-0057-0
27. Charrois GJ, Allen TM (2003) Multiple injections of pegylated liposomal doxorubicin: pharmacokinetics and therapeutic activity. J Pharmacol Exp Ther 306(3):1058–1067. doi:10.1124/jpet.103.053413
28. Caron WP, Song G, Kumar P, Rawal S, Zamboni WC (2012) Interpatient pharmacokinetic and pharmacodynamic variability of carrier-mediated anticancer agents. CPT Pharmacomet Syst Pharmacol 91(5):802–812. doi:10.1038/clpt.2012.12
29. Zamboni WC, Maruca LJ, Strychor S, Zamboni BA, Ramalingam S, Edwards RP, Kim JK, Bang YJ, Lee HY, Friedland DM (2011) Bidirectional pharmacodynamic interaction between pegylated liposomal CKD-602 (S-CKD602) and monocytes in patients with refractory solid tumors. J Liposome Res 21(2):158–165
30. Zamboni WC, Eiseman JL, Strychor S, Rice PM, Joseph E, Zamboni BA, Donnelly MK, Shurer J, Parise RA, Tonda ME (2011) Tumor disposition of pegylated liposomal CKD-602 and the reticuloendothelial system in preclinical tumor models. J Liposome Res 21(1):70–80
31. La-Beck NM, Zamboni BA, Gabizon A, Schmeeda H, Amantea M, Gehrig PA, Zamboni WC (2012) Factors affecting the pharmacokinetics of pegylated liposomal doxorubicin in patients. Cancer Chemother Pharmacol 69(1):43–50. doi:10.1007/s00280-011-1664-2
32. Coleman RE, Blinder RA, Jaszczak RJ (1986) Single photon emission computed tomography (SPECT). Part II: clinical applications. Invest Radiol 21(1):1–11
33. Gabizon A, Isacson R, Rosengarten O, Tzemach D, Shmeeda H, Sapir R (2008) An open-label study to evaluate dose and cycle dependence of the pharmacokinetics of pegylated liposomal doxorubicin. Cancer Chemother Pharmacol 61(4):695–702. doi:10.1007/s00280-007-0525-5
34. Zamboni WC, Ramalingam S, Friedland DM, Edwards RP, Stoller RG, Strychor S, Maruca L, Zamboni BA, Belani CP, Ramanathan RK (2009) Phase I and pharmacokinetic study of pegylated liposomal CKD-602 in patients with advanced malignancies. Clin Cancer Res 15(4):1466–1472. doi:10.1158/1078-0432.CCR-08-1405
35. Zamboni WC, Strychor S, Maruca L, Ramalingam S, Zamboni BA, Wu H, Friedland DM, Edwards RP, Stoller RG, Belani CP (2009) Pharmacokinetic study of pegylated liposomal CKD-602 (S-CKD602) in patients with advanced malignancies. CPT Pharmacomet Syst Pharmacol 86(5):519–526
36. Nielsen H (1984) Effect of cis-platinum on human blood monocyte function in vitro. Cancer Immunol Immunother (CII) 18(3):223–225
37. Skelton H, Linstrum J, Smith K (2002) Host-vs.-altered-host eruptions in patients on liposomal doxorubicin. J Cutan Pathol 29(3):148–153. doi:10.1034/j.1600-0560.2002.290304.x
38. Richardson DS, Johnson SA (1997) Anthracyclines in haematology: preclinical studies, toxicity and delivery systems. Blood Rev 11(4):201–223